Prediction of near wall turbulence using minimal flow units and application

Guang Yin
Department of Engineering Mechanics
Tsinghua University
Beijing, China
ying13@mails.tsinghua.edu.cn

W.-X. Huang
Department of Engineering Mechanics
Tsinghua University
Beijing, China
hwx@tsinghua.edu.cn

C.-X. Xu
Department of Engineering Mechanics
Tsinghua University
Beijing, China
xucx@tsinghua.edu.cn

ABSTRACT

In the present study the near-wall behaviour of turbulent channel flow at $Re_\tau = 1000, 2000$ is investigated in the minimal domain designed to maintain healthy turbulence up to $y^+ \approx 100$. The minimal flow units can reproduce statistical behaviour of small-scale motions in the full-sized channel in the absence of outer motions, which implies that the minimal flow unit could embody the universal properties of near-wall turbulence.

Furthermore, combined with the signals of outer large-scale motions, the signals extracted from the minimal channels are used to predict the near-wall turbulence fluctuations in the full-sized channel and build the off-wall boundary conditions for the large-eddy simulation in the outer region.

INTRODUCTION

A great number of studies in the last decades have been conducted to understand the mechanism of near-wall turbulence. It is now well accepted that the self-sustaining process (SSP) of streaks and quasi-streamwise vortices plays an important role in the buffer layer (Hamilton et al. 1995). Recent researches have revealed that the SSP can also exist in log-layer and in larger-scale motions after artificially damping motions with smaller scales in lower normal region (Hwang & Cossu 2010). These larger-scale self-sustaining structures are self-similar belonging to a hierarchy of attached eddies (Hwang et al. 2015), which are in consistence with the attached eddy hypothesis (Townsend 1976). The attached eddies contain streaky structures and vortical structures at different length scales. A series of minimal computational domains can be used to isolate these structures to study a single or several coherent structures. In Flores & Jiménez (2010), it is stated that in order to maintain a 'healthy' turbulence beneath y_h^+, the minimal spanwise width of the boxes should satisfy $L_z^+ \approx 3y_h^+$. Additionally, Hwang (2013, 2015) designed a numerical spanwise-average filter to further remove the influence of the outer motions and used over-damping LES to isolate the attached eddies at a prescribed length scales. All these studies are aimed to investigate statistical as well as dynamical properties of the near-wall coherent structures in the minimal flow units (MFU) because of their low dimensions.

Although the minimal flow unit can serve as a reduced-order model in representing the near-wall turbulence to some extent, the turbulence intensities obtained in MFU are still less than those in the full-sized channel. Furthermore, with increasing Reynolds number, the interactions between near-wall fluctuations and outer large-scale motions are becoming intense (Hutchins et al. 2007, Marusic et al. 2010). A simple mathematical model is proposed to quantitatively account for the influence of outer large-scale motions on the near-wall fluctuations (Marusic et al. 2010). In the present study, the model is revised to combine with the minimal flow units in predicting the near-wall turbulent behaviour, which is then used as the off-wall boundary conditions for the full-sized simulations at moderate Reynolds number ($Re_\tau \sim O(1000)$) to save computational cost.

NUMERICAL METHOD

DNS is used to investigate the near-wall behaviour of MFU at $Re_\tau = 1000,2000$. Fourier-Galerkin method is adopted to discretize the periodic streamwise x and spanwise z direction and the fourth-order compact finite difference scheme is used for discretization in the wall-normal y direction. Spanwise-average filter is conducted by setting the right-hand-side terms for spanwise wavenumber $k_z = 0$ to be zero in the streamwise and

wall-normal momentum equations during temporal integration as used in Hwang (2013). The streamwise and spanwise sizes of the computational boxes are $(L_x^+, L_z^+) \approx (3000,300)$ so as to maintain healthy turbulence below $y^+ \approx 100$. Further tests of the MFU used as off- wall boundary condition are conducted by LES in the full-sized domain of $(L_x, L_y, L_z) \approx (8\pi, 2,3\pi)h$ (h denotes the half height of the channel) at $Re_\tau = 1000$, where the boundary condition for the three components are synthesized by MFU near the lower boundary of log-layer, $y^+ \approx 10$. Dynamical Smagorinsky model is used to close the sub-grid stresses.

RESULTS

Parameters in the predictive model

The predictive models used in the present work takes the form of

$$u_p^+(y^+) = u_{\min}^+(y^+)[1 + \beta_u u_{OL}^+] + \alpha_u u_{OL}^+ \qquad (1)$$

which is similar to the model used in Marusic et al. (2010)

$$u_p^+(y^+) = u^*(y^+)[1 + \beta_u u_{OL}^+] + \alpha_u u_{OL}^+ \qquad (2)$$

but uses fluctuation signals extracted from MFU to surrogate the original universal signals in (2). Since the universal signals are shielded from the influence of the outer large-scale motions, they share similar properties to the near-wall velocity fluctuation in the MFU. The superposition and modulation coefficients are calculated from the full-sized DNS data at $Re_\tau = 1000$ (Deng 2014) and $Re_\tau = 2003$ (Hoyas & Jiménez 2008).

In the experiments of Marusic et al. (2010), the large-scale input signals u_{OL}^+ at the center of log-layer region $y_O^+ = 3.9\sqrt{Re_\tau}$ are retained by filtering the original signals larger than the streamwise cutoff wavelength of $\lambda_x^+ \approx 7000$, which is the streamwise length to separate the inner and outer peak in the premultiplied streamwise energy spectra (Hutchins et al. 2007). Then, due to the angle of the coherent structures θ_L, the large-scale signals have to be shifted Δx in the streamwise direction to account for the largest cross-correlation of the large-scale signals between the log-layer and the near-wall region and the superposition coefficients at y^+ is defined as the maximum correlation:

$$\alpha = R\{u_{OL}^+(y_O^+, t), u_O^+(y^+, t)\} \qquad (3)$$

where u_O^+ denotes large scale near wall region filtered by the same length as at the log-layer center. Because of the access to the three dimensional flow field data of direct numerical simulation, the filtering to obtain large-scale motions can be conducted both in the streamwise and spanwise direction and the cutoff wavelength is chosen to approximate the size of the minimal channel boxes of $(L_x^+, L_z^+) \approx (3000,300)$.

The superposition coefficients, at the wall-normal locations between $10 \le y^+ \le 100$ as well as the incline angle of the large-scale structures:

$$\theta_L = \arctan\left((y_O^+ - y^+)/\Delta x_m\right) \qquad (4)$$

where Δx_m is the streamwise shift corresponding to the maximum cross correlation, are displayed in Figure.1 (a), (b) at the two Reynolds number. The range of the angle is $11^o \sim 20^o$ in agreement to Marusic et al. (2010), Mathis et al. (2011), as also included in the Figure. 1 (b). The value of the superposition coefficients becomes larger with closer distance to the center of log-layer where u_{OL}^+ is obtained. It seems that the correlation of $Re_\tau = 2003$ is relatively smaller than that of $Re_\tau = 1000$, which may be due to the higher location of the log-layer center at higher Reynolds number. The value of correlation between large-scale motions is dependent on the cutoff wavelength, the superposition coefficients are different from Mathis et al. (2011).

The modulation effects of u_{OL}^+ are represented by the first term of RHS in (1) and β is the modulation coefficient calculated through the iterative procedure to get the de-modulation universal signal u^* which satisfies:

$$\mathrm{AM}(u^*) = 0 \qquad (5)$$

known as:

$$\mathrm{AM}(u^*) = (\langle H_L(u^*) u_{OL}^+ \rangle) / \sqrt{\langle u^* u^* \rangle \langle u_{OL}^+ u_{OL}^+ \rangle} \qquad (6)$$

'$\langle \ldots \rangle$' denotes spatial and temporal average and $H_L(..)$ denotes the filtered Hilbert transformation of signals. AM can be used to quantify the degree of the modulation effects of the log-layer large-scale signals on the near-wall velocity fluctuations. Figure. 1(b) shows the modulation coefficients in variance with the normal location for the two Reynolds numbers. Obviously β increases with higher Reynolds number indicating the stronger degree of amplitude modulation.

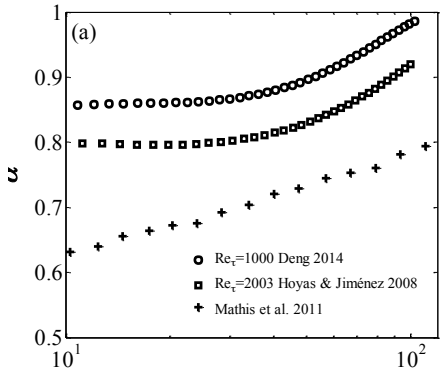

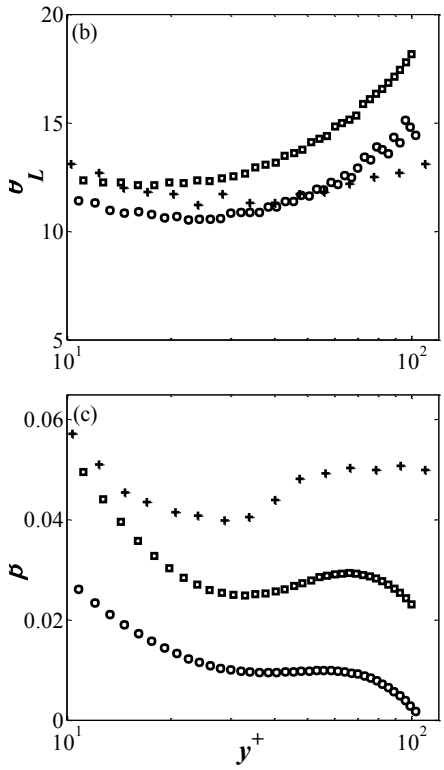

Figure 1. The parameters in the predictive model (a) the superposition coefficients. (b) the incline angles of the large-scale structures. (c) the modulation coefficients within $10 \leq y^+ \leq 100$ of the two Reynolds numbers in the present study compared with turbulent boudnary layer at $Re_\tau = 7300$ in Mathis et al. 2011.

Prediction of the near-wall turbulence using MFU

In practice by using the model (1), the minimal flow unit is replicated periodically in the streamwise and spanwise direction so that the velocity fluctuations at a specific wavenumber in the minimal flow unit are implemented at the same wavelength in the full-sized channel. In this way the small-scale de-modulated motions in the full-sized channel are reproduced by the minimal flow unit and the self-sustaining dynamics of the near-wall streaks and the quasi-streamwise vortices in the real turbulence can be modeled. Nevertheless, it imposes artificial periodicity and the amplitude on some Fourier wavenumbers may be zeros, the statistical features are not influenced significantly (Mizuno & Jiménez 2013, R. Garcia-Mayoral et al. 2013) except for the high moments of the velocity fluctuations, which is not the aim of the present study. The procedure is briefly outlined in Figure 2. The outer large-scale structures from the centre of the log-layer in the full-sized DNS are used to quantify the interaction between inner layer and outer layer in the predictive model.

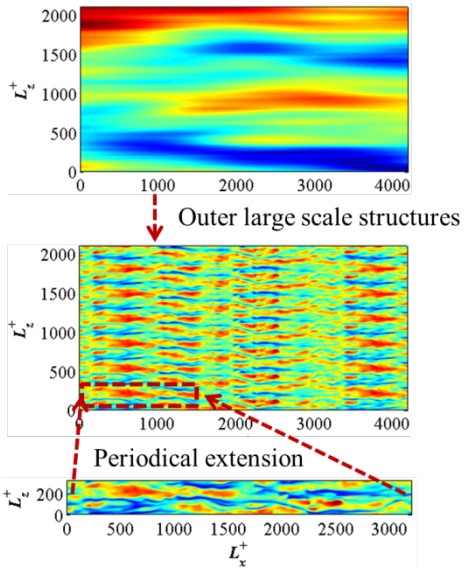

Figure 2. Periodic extension of MFU to the full-sized channel (1/144 of the full-sized plane is displayed) at $Re_\tau = 2000$. The plane outer large-scale structures are extracted from full-sized DNS at $Re_\tau = 2003$ (Hoyas & Jiménez 2008).

The prediction of the near-wall streamwise velocity fluctuation u using MFU signals are displayed in Figure 3 and 4 for the second- and third-order moments. It can be seen that $\langle uu \rangle^+$ of MFU at the considered Reynolds number are lower than the full-sized channels but the predicted turbulence intensities show good agreement with the full-sized simulation (Deng 2014, Hoyas & Jiménez 2008) due to the inclusion of linear superstition of the log-layer large-scale motions.

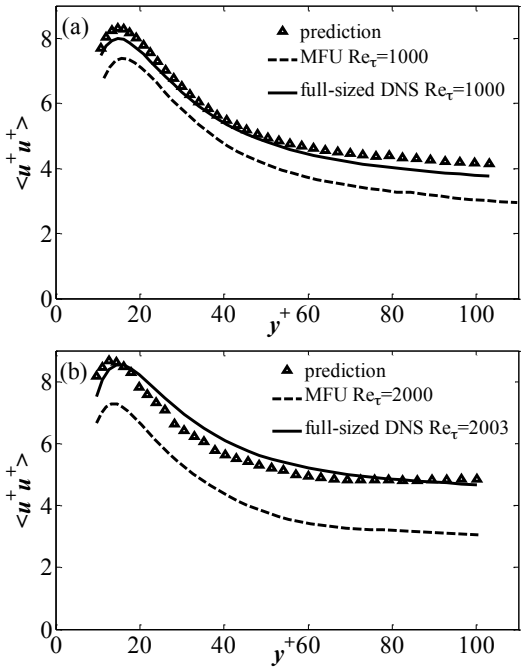

Figure 3. Profiles of $\langle uu \rangle^+$. (a) $Re_\tau = 1000$ and (b) $Re_\tau = 2003$.

In addition, the 3rd order moments are well predicted within the near-wall region as shown in Figure 4, showing the effects of modulation of large-scale motions.

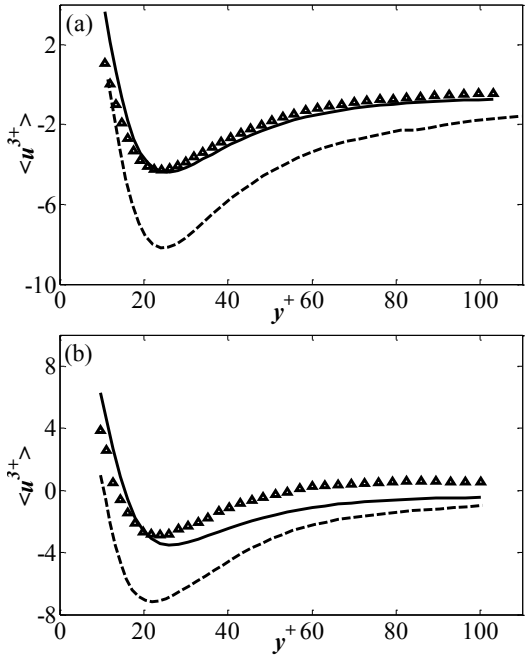

Figure 4. Profiles of $\langle u^3 \rangle^+$. (a) $Re_\tau = 1000$ and (b) $Re_\tau = 2003$. See Figure. 3 for the legend.

The prediction of spanwise velocity component w is also studied at $Re_\tau = 1000$ in the present work because it belongs to the attached variables and is under the influence of the outer large-scale structures (The wall normal component is detach variables and preliminary tests confirm $\langle vv \rangle^+$ in the MFU is almost the same as in full-sized DNS). It is implicated by the three dimensional conditional structures that the spanwise velocity fluctuations within the near-wall region can be predicted in the similar way as the streamwise velocity fluctuations (Talluru et al. 2014). The superstition of the streamwise large-scale signals at the center of the log-layer is considered. However as the large-scale streamwise structures locate between the three-dimensional conditional counter-rotating roll-modes, spanwise shifts have to be taken in account. Figure 5 shows that after adding the linear superposition of streamwise component of the log-layer large-scale motions, the turbulence intensity agrees well with the full-sized simulation.

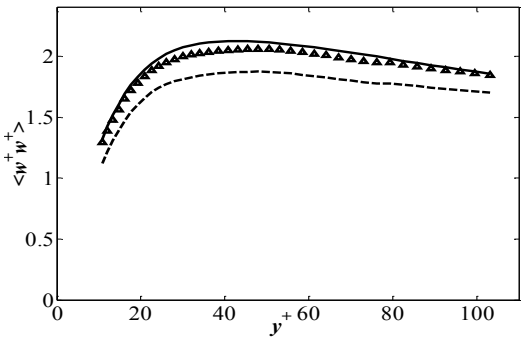

Figure 5. Profiles of $\langle ww \rangle^+$ at $Re_\tau = 1000$. For lengend see Figure. 3.

OFF-WALL BOUNDARY CONDITION USING THE PREDICTIVE MODEL

For practical application, the present study extracts the velocity fluctuations in MFU to form the off-wall boundary conditions for the LES in the full-sized channel. Similar work has been conducted by Mayoral et al. (2013), in which velocity fluctuations from turbulent spots in transitional boundary layer were employed to synthesize the boundary condition. However this method is only tested at relative low-Reynolds number and is in the absence of the outer influence. In the present study, the simulation is conducted above off-wall boundary plane around $y^+ \approx 100$.

The same procedure as in Figure 2 is conducted during simulation. At every time step, large-scale streamwise signals from the centre of the above log-layer serve as input to account for the footprint of outer motions on off-wall boundary.

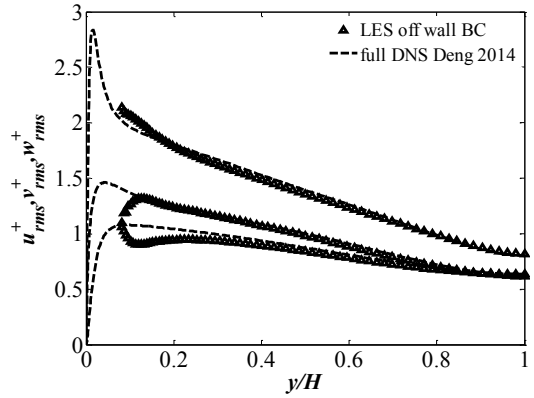

Figure 6. Root-mean square of velocity fluctuations by LES using off-wall boundary condition and DNS (Deng 2014) at $Re_\tau = 1000$.

The resulting root-mean squares of the three velocity components are displayed in Figure 7. The fluctuations in the outer region of the channel show excellent agreement with DNS result (Deng 2014). The energy of streamwise velocity at the boundary is also equal to the full DNS proving the influence of the outer motions. The little flaw lies in the adaption region

between the off-wall boundary and the upper layer, also reported by Mizuno et al (2013) and Mayoral et al (2013). One dimensional spanwise energy spectra of u in Figure 6 shows that although there is discreteness due to periodic blocks (Mizuno et al. 2013), the overall energy distribution agree well with DNS and there appears the outer peak of large-scale structures.

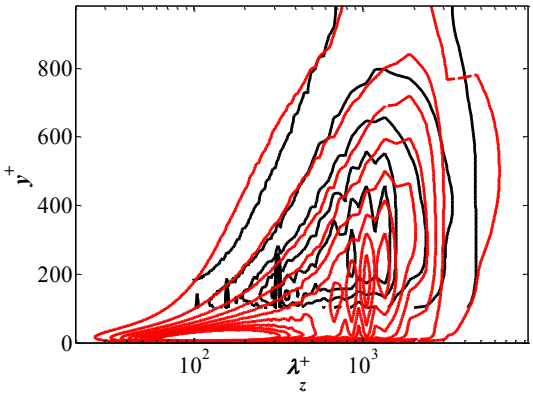

Figure 7. One-dimensional spanwise spectra of streamwise velocity. Black: LES using off wall boundary condition; Red: full-sized DNS at $Re_\tau = 1000$ (Deng 2014).

CONCLUSION

The present study firstly takes advantage of the velocity fluctuation in the minimal flow unit with the predictive model (Marusic et al. 2010, Mathis et al. 2011) to obtain the near-wall statistics in the full-sized turbulent channel flow. The log-layer large-scale motions are filtered at the same length scales as the sizes of the MFU from direct numerical simulation data at $Re_\tau = 1000$ and $Re_\tau = 2003$ to be the input of the predictive model. The superposition and modulation coefficients in the predictive model are yielded using the three dimensional DNS data.

The near-wall small-scale motions are reproduced by periodically replicating the MFU both in streamwise direction and the spanwise direction and the influence of the outer large-scale motions is included as in the model (2). The gap of 2nd order moment or turbulence intensity between MFU and the full-sized turbulent channel is fixed owe to the superposition effects and 3rd order moment is better predicted by adding the amplitude modulation effects of the large-scale motions. For the prediction of the spanwise velocity fluctuation, the same model is used and the turbulence intensity displays good agreement with that of the full-sized turbulent channel flow. The wall-normal fluctuation in MFU is already sufficient to reproduce the near-wall statistics of the full-sized turbulent channel flow because there is little energy contained in large scale range in the component.

The predictive model in the present study is used as the off-wall boundary condition in LES of the full-sized channel flow at $Re_\tau = 1000$. The turbulence intensities of velocity fluctuations in the outer region show excellent agreement with DNS and the one-dimensional spanwise energy spectra shows that the outer large-scale structures are produced. However there still remain some shortcomings with the wall model. For instance the turbulence intensities display regions of high fluctuation close to the location of the off-wall boundary and the effects of artificial periodical replication of MFU can reach into the outer region as indicated by the energy spectra.

Further research to extent the model to higher Reynolds numbers and to raise the normal position of the off-wall boundary to further reduce the computational cost is our future work.

REFERENCES

Deng B Q. 2014 Research on mechanism of drag-reduction control based on coherent structures in wall-turbulence. [PhD Thesis]. Beijing: School of Aerospace Engineering, Tsinghua University.

Flores O, Jiménez J. 2010 Hierarchy of minimal flow units in the logarithmic layer. Physics of Fluids 22(7): 071704.

Garcia-Mayoral R, Pierce B, Wallace J M. Off-wall boundary conditions for turbulent simulations from minimal flow units in transitional boundary layers[C]//TSFP DIGITAL LIBRARY ONLINE. Begel House Inc., 2013.

Hamilton, J. M., Kim, J., & Waleffe, F. 1995 Regeneration mechanisms of near-wall turbulence structures. Journal of Fluid Mechanics, 287, 317-348.

Hoyas S, Jiménez J. 2008 Reynolds number effects on the Reynolds-stress budgets in turbulent channels. Physics of Fluids 20(10): 101511.

Hutchins N, Marusic I. 2007 Large-scale influences in near-wall turbulence. Philosophical Transactions of the Royal Society of London A: Mathematical, Physical and Engineering Sciences 365(1852): 647-664.

Hwang Y. 2013 Near-wall turbulent fluctuations in the absence of wide outer motions. Journal of Fluid Mechanics 723: 264-288.

Hwang Y. 2015 Statistical structure of self-sustaining attached eddies in turbulent channel flow. Journal of Fluid Mechanics 767: 254-289.

Hwang Y, Cossu C. 2010 Self-sustained process at large scales in turbulent channel flow. Physical Review Letters 105(4): 044505.

Marusic I, Mathis R, Hutchins N. 2010 Predictive model for wall-bounded turbulent flow. Science 329(5988): 193-196.

Mathis R, Hutchins N, Marusic I. 2011 A predictive inner–outer model for streamwise turbulence statistics in wall-bounded flows. Journal of Fluid Mechanics 681: 537-566.

Mizuno, Y., & Jiménez, J. 2013 Wall turbulence without walls. Journal of Fluid Mechanics, 723, 429-455.

Talluru, K. M., Baidya, R., Hutchins, N., & Marusic, I. 2014 Amplitude modulation of all three velocity components in turbulent boundary layers. Journal of Fluid Mechanics, 746, R1.

Townsend AA. 1976 The structure of turbulent shear flow. Cambridge university press.